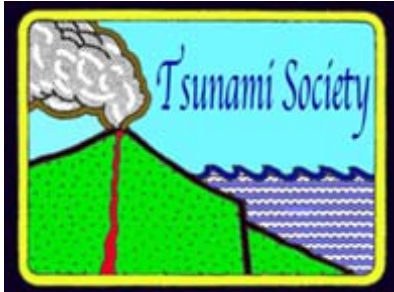


ISSN 8755-6839



## SCIENCE OF TSUNAMI HAZARDS

---

Journal of Tsunami Society International

Volume 36

Number 2

2017

---

### NUMERICAL MODELING OF MOON ASTEROID IMPACTS TSUNAMIS ON THE MOON

Charles L. Mader

*Mader Consulting Co.  
Honolulu, HI 96825 U.S.A.*

#### ABSTRACT

Asteroid impacts on the moon were modeled using the full Navier-Stokes AMR Eulerian compressible hydrodynamic code called MAGNS. The size of the cavity and its time history are strongly dependent upon the strength characteristics of the moon rock. The initial impact pressures and temperatures are well above shock melting conditions at the impact surface of the moon.

The formation of a moon crater, its rings and mascon is modeled.

**Keywords:** *Modeling, Navier-Stokes, Eulerian, moon crater, crater rings.*

*Vol 36. No. 2, page 49 (2017)*

## INTRODUCTION

William Van Dorn has proposed models to explain the observed rings in the craters on the moon as described in (Van Dorn, 1968 and 1969) which he calls "Tsunamis on the Moon." He requested modeling of the impact of a 10-kilometer radius basalt or iron asteroid moving at 10 kilometers/second with the moon assuming possible liquid and solid basalt layers.

## 1 NUMERICAL MODELING

The compressible Navier-Stokes equations are described in (Mader, 2004, 1998) and examples of many numerical solutions of complicated physical problems are described. The compressible Navier-Stokes equations are solved by a high-resolution Godunov differencing scheme using an adaptive grid technique described in (Gittings, 1992).

The solution technique uses Continuous Adaptive Mesh Refinement (CAMR). The decision to refine the grid is made cell-by-cell continuously throughout the calculation. The computing is concentrated on the regions of the problem, which require high resolution.

Refinement occurs when gradients in physical properties (density, pressure, temperature, material constitution) exceed defined limits, down to a specified minimum cell size for each material. The mesh refinement is described in detail in (Mader, 2004).

Much larger computational volumes, times and differences in scale can be simulated than possible using previous Eulerian techniques such as those described in (Mader, 1998).

The original code was called SAGE. A later version with radiation is called RAGE. A recent version with the techniques for modeling reactive flow described in (Mader, 2004) is called NOBEL.

Some of the remarkable advances in fluid physics using the NOBEL code have been the modeling of Richtmyer-Meshkov and shock induced instabilities described in (Holmes et al., 1999 and Baltrusaitis et al., 1996). It was used for modeling the Lituya Bay impact landslide generated tsunami and water cavity generation described in (Mader 1999 and 2002). NOBEL/SAGE/RAGE were used to model the generation of water cavities by projectiles and explosions and the resulting water waves in (Mader and Gittings, 2003). The codes were used to model asteroid impacts with the ocean and the resulting tsunami waves in (Gisler, et al., 2003, 2004).

The codes can describe one-dimensional slab or spherical geometry, two-dimensional slab or cylindrical geometry, and three-dimensional Cartesian geometry.

Because modern supercomputing is currently done on clusters of machines containing many identical processors, the parallel implementation of the code is very important. For portability and scalability, the codes use the Message Passing Interface (MPI). Load leveling is accomplished through the use of an adaptive cell pointer list; in which newly created daughter cells are placed immediately after the mother cells. Cells are redistributed among processors at every time step, while keeping mothers and daughters together. If there are a total of M cells and N processors, this technique gives nearly  $(M / N)$  cells per processor. As neighbor cell variables are needed, the MPI gather/scatter routines copy those neighbor variables into local scratch memory.

The calculations described in this paper were performed on IMAC Apple and PC computers and did not require massive parallel computers.

The codes incorporate multiple material equations of state (analytical or SESAME tabular). Every cell can in principle contain a mixture of all the materials in a problem assuming that they are in pressure and temperature equilibrium.

As described in (Mader, 1998), pressure and temperature equilibrium is appropriate only for materials mixed molecularly. The assumption of temperature equilibrium is inappropriate for mixed cells with interfaces between different materials. The errors increase with increasing density differences. While the mixture equations of state described in (Mader, 1998) would be more realistic, the problem is minimized by using fine numerical resolution at interfaces. The amount of mass in mixed cells is kept small resulting in small errors being introduced by the temperature equilibrium assumption.

Very important for late time cavity history is the capability to initialize gravity properly, which is included in the code. This results in the initial density and initial pressure-changing going from the very low-density atmosphere at 20 kilometers altitude down to the moon surface. Likewise the rock density and pressure changes correctly with increasing depth. The moon gravity constant used was 167 vs 980 for the earth.

Soon after the initial impact and the cavity formation is occurring, the previously shocked and compressed rock is being rarefied and pulverized. The rock is called “fluidized” and modeled as described in the modeling of crater formation of the Arizona meteor crater and the SEDAN nuclear crater described in (Mader, 2009).

A new code called MAGNS was used in this study. It has been used to model oblique shock initiation of insensitive explosives described in (Mader and Gittings, 2004).

#### SUMMARY OF MODELED CAVITY DIMENSIONS

For a 20 kilometer diameter Projectile impacting Moon Crust at 10 kilometer/sec

Problem	Max Depth	Max Diameter	Collapse
Basalt Projectile, 5.5 kb Basalt Yield	40 km	60 km	No
Iron Projectile, 5.5 KB Basalt Yield	80 km	90 km	No
Basalt Projectile, Fluid Basalt	- 1000 s 75 km	120 km	Yes
	- 2000 s 70 km	160 km	
	- 3000 s 30 km	180 km	Axis Jet
Basalt projectile, impacts water	- 1000 s 120 km	120 km	Yes
	- 2000 s 100 km	160 km	
	- 3000 s Axis Jet	180 km	

The cavity formed by an asteroid impact on the moon is strongly dependent upon the strength characteristics of the moon rock and whether it is described as a solid with strength or a fluid without strength. With sufficient strength the cavity grows to a maximum size and no axis jet is formed. The size of the cavity is strongly dependent upon the density of the asteroid and its velocity. The initial impact pressures and temperatures are well above shock melting conditions at the impact surface of the moon. The impact pressure for the basalt projectile is greater than 1 megabar, the impact density is greater than 5 g/cc, and the impact temperature is greater than 6000 K. The initial impact pressure for the iron projectile is greater than 1.5 megabar and the iron impact density is greater than 11 grams/cc.

Soon after the initial impact and the cavity formation is occurring, the previously shocked and compressed rock is being rarefied and pulverized. The rock is called “fluidized” and modeled as described in the modeling of crater formation of the Arizona meteor crater and the SEDAN nuclear crater.



### **Mare Orientale**

*NASA, Lunar Orbiter 4*

900 km across

Collision caused ripples in the lunar crust resulting in three (5 according to Van Dorn)

concentric circular ring like features.

It is relatively unflooded by mare basalts.

The outermost ring is 930 km in diameter with ejecta extending 500 km beyond.

Figure 1. The mare Orientale photographed by Lunar Orbiter 4.

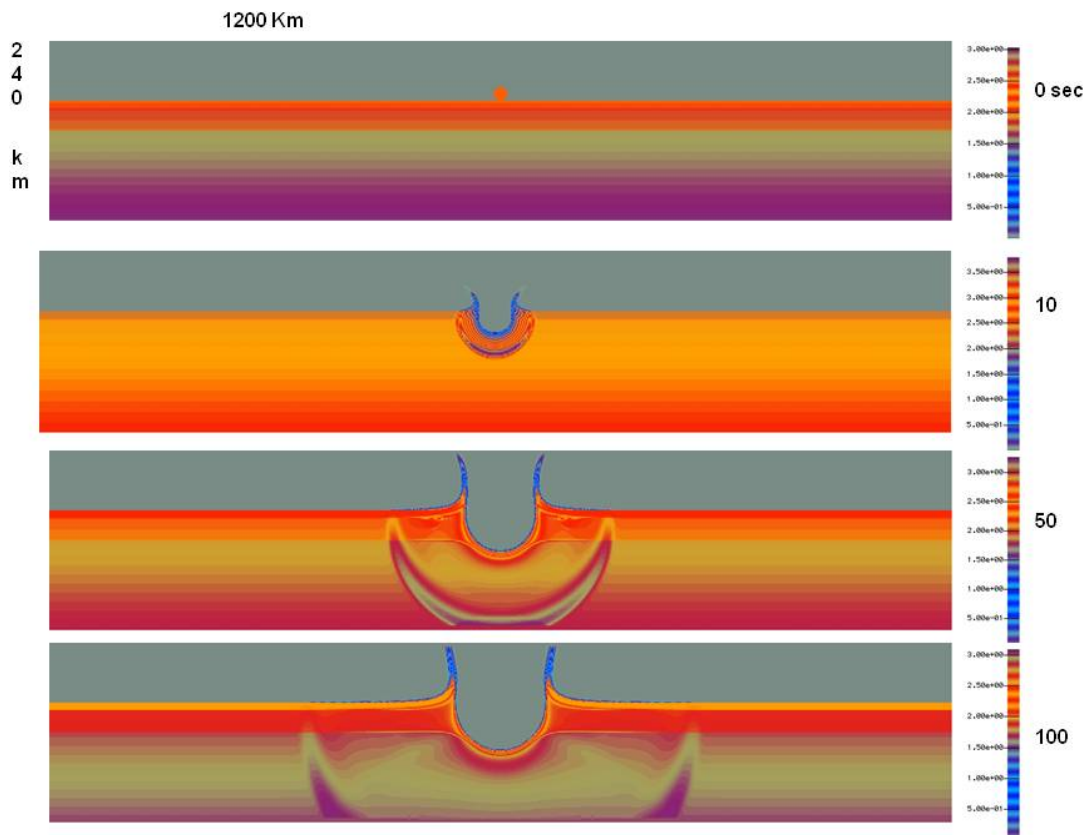
The moon crater formation by an asteroid impact was modeled for a 1200 and 800 kilometer diameter block of Basalt, 160 kilometer thick. Above the Basalt was 80 kilometers of void making the problem 240 kilometers high. The geometry was cylindrical with the projectile impacting on the

cylindrical axis. The gravity constant for the moon used was 167, which compares with 980 for the earth.

MAGNS was used to model the impact of a 10 kilometer diameter Iron Asteroid moving at 10 kilometers/sec with 10 kilometer thick Basalt Crust at 2.86 g/cc, 30 kilometer thick Basalt Mare at 3.10 g/cc and 120 kilometer thick Basalt Mantel at 3.31 g/cc. The basalt yield was 0.01 kilobar. Similar results were obtained for basalt yields up to 0.1 kilobar.

The density contours are shown for the first hour after impact in Figure 2. The times are in seconds. After the moon cavity, rings and mascon have been formed the density, pressure and velocity in the Y direction contours are shown for 800 kilometer diameter in Figure 3 and compared with the Orientale crater in Figure 4 using the Van Dorn locations of the rings.

A PowerPoint and movies are available at [www.mccoehi.com/moon/moon.htm](http://www.mccoehi.com/moon/moon.htm) .



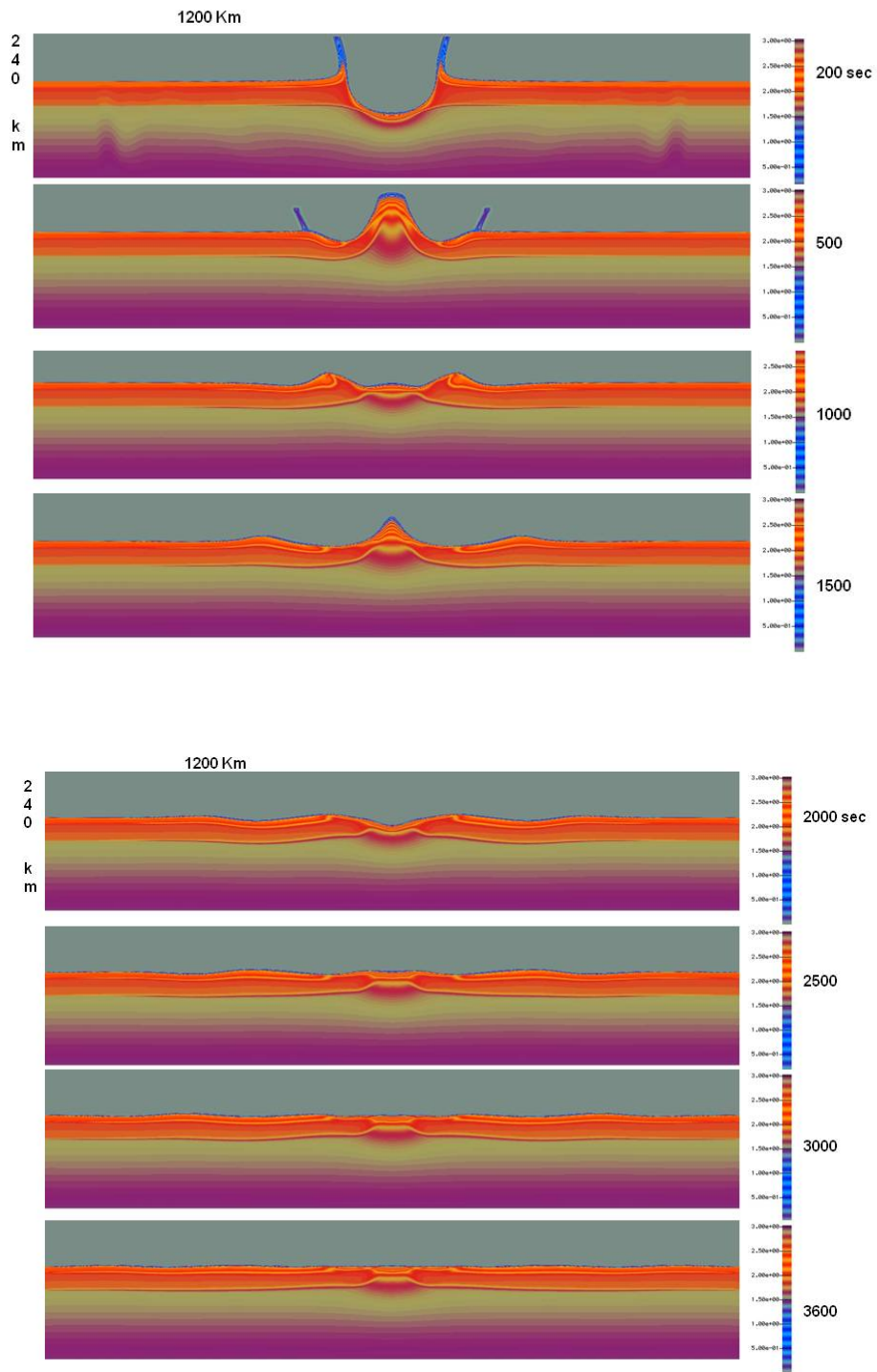


Figure 2. The density contours for a 1200-kilometer diameter block of Basalt impacted by a 10 kilometer diameter Iron Asteroid moving at 10 kilometer/sec.

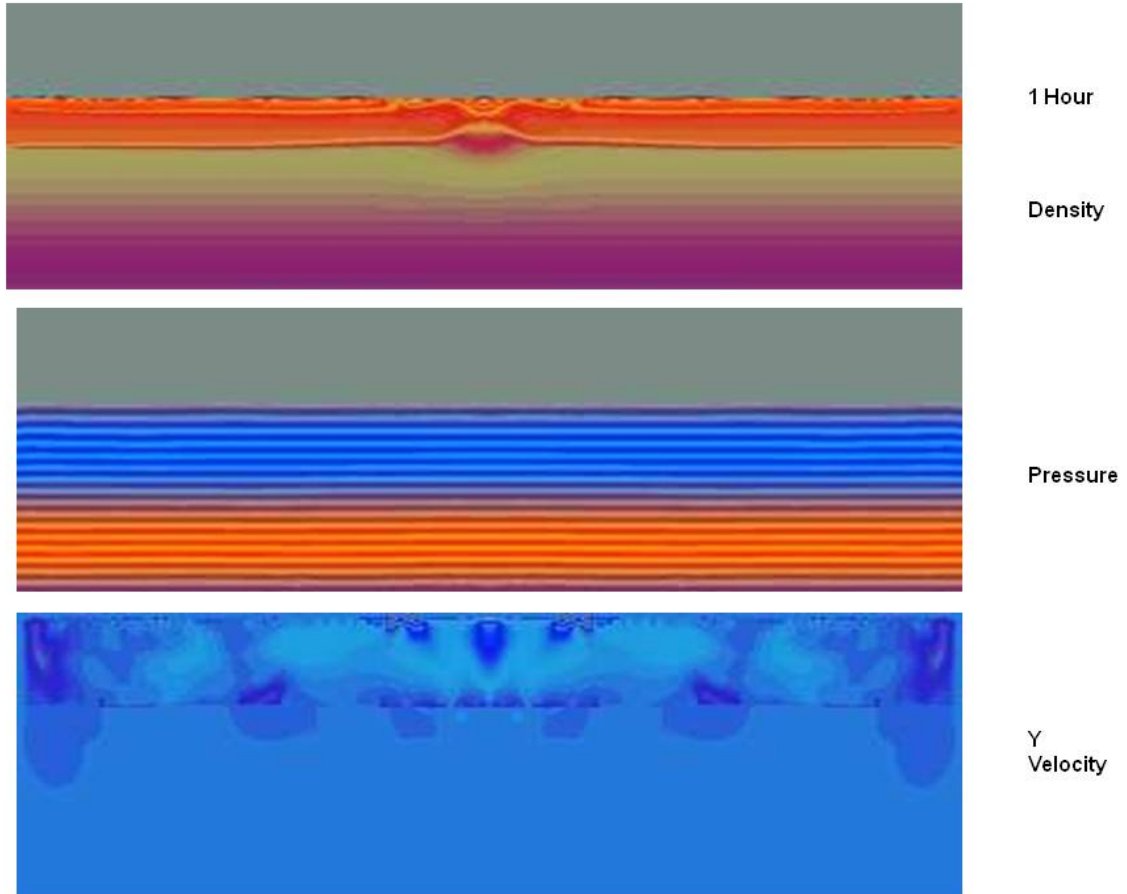
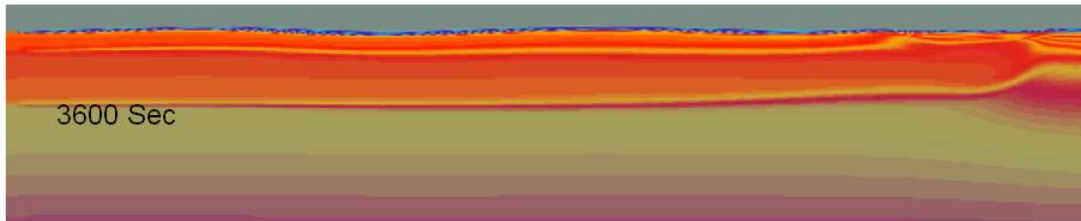


Figure 3. The density, pressure and velocity in the Y direction contours, 3600 seconds after a 800-kilometer diameter block of Basalt is impacted by a 10 kilometer diameter asteroid moving at 10 kilometers/second.

Cavity Diameter - 100 sec 120 km **Orientele 136 km**  
 130 130  
 At Max Depth 150 140  
 200 150 - Cavity Depth Decreasing



0 km Ht	1	-2	1	-1	1	-4	1
595 km	495	380	270	170	115	65	0
	100	115	110	100	65	55	

**Orientele Crater Ring Peak Locations and Heights at 62 minutes Freeze Time**

680	465	310	240	180
0.5	1.5	3.0	2.5	0.5

Figure 4. The density profile at 3600 seconds for a 600-kilometer radius Basalt block with the height and radius of the calculated maximum and minimum crater rings and distances between the maximum and minimum shown in black. The Van Dorn Orientele peak crater ring locations and heights are shown in red. The calculated maximum crater diameter at various times is shown at the top of the figure.

The number of rings and their locations and heights as determined by Van Dorn are not accurately modeled. Modeling the moon as a flat cylinder instead of a sphere may be a major source of the failure to describe the Orientele rings. The fluidization model and its calibration may also contribute to the failure to describe the Orientele ring number, locations and heights. The number of rings and their location and heights is also difficult to evaluate accurately from the available photographs. The size and velocity of the asteroid is also unknown. The Van Dorn published mechanism for the formation of the rings, his "Tsunamis on the Moon" is supported by the modeling. The tsunami wave occurred in molten and pulverized rock instead of water.



## ACKNOWLEDGMENTS

The contributions of Dr. William Van Dorn, Dr. Rob Coker and Dr. Galen Gisler are gratefully acknowledged.

## REFERENCES

1. Van Dorn, W., 1968, Tsunamis on the Moon?. *Nature*, v. 220, No. 5172, p. 1102-1107.
2. Van Dorn, W., 1969, Lunar Mare Structure and Evolution. *Science*, v. 165, p. 603-695.
3. Mader, C.L., 2004, **Numerical Modeling of Water Waves- Second Edition**, CRC Press, Boca Raton, Florida.
4. Mader, C.L., \1998, **Numerical Modeling of Explosives and Propellants**, CRC Press, Boca Raton, Florida.
5. Gittings, M.L., 1992, SAIC's Adaptive Grid Eulerian Code, Defense Nuclear Agency Numerical Methods Symposium, p. 28-30.
6. Holmes, R.L., Dimonte, G., Fryxell, B., Gittings, M.L., Grove, J.W. Schneider, M., Sharp, D.H., Velikovich, A.L., Weaver, R.P., and Zhang, Q., 1999, Richtmyer-Meshkov Instability Growth: Experiment, Simulation and Theory, *Journal of Fluid Mechanics*, v. 9, p. 55-79.
7. Baltrusaitis, R.M., Gittings, M.L., Weaver, R.P., Benjamin, R.F., and Budzinski, J.M., 1996, Simulation of Shock-Generated Instabilities, *Physics of Fluids*, v. 8, p. 2471-2483.
8. Mader, C.L., 1999, Modeling the 1958 Lituya Bay Tsunami, *Science of Tsunami Hazards*, v. 17, p. 57-67.
9. Mader, C.L., 2002, Modeling the 1958 Lituya Bay Mega-Tsunami, II, *Science of Tsunami Hazards*, v. 20, p. 241-250.
10. Mader, C.L., and Gittings, M.L., 2003, Dynamics of Water Cavity Generation, *Science of Tsunami Hazards*, v. 21, p. 91-118.
11. Gisler, G., Weaver, R., Gittings, M.L. and Mader, C., 2003, Two- and Three-Dimensional Simulations of Asteroid Ocean Impacts, *Science of Tsunami Hazards*, v. 21, p. 119-134.

12. Gisler, G., Weaver, R., Gittings, M.L. and Mader, C., 2004, Two- and Three-Dimensional Asteroid Impact Simulations, Computers in Science and Engineering.
13. Charles L. Mader, C.L., 2009, Numerical Modeling of Crater Formation by Meteorite Impact and Nuclear Explosion, PREDICTIVE MODELING OF DYNAMIC PROCESSES, p. 447-457, Springer.
14. Mader, C.L. and Michael Gittings, M., 2004, Numerical Modeling of Oblique Initiation of Insensitive High Explosives, [www.mccohi.com/oblique/oblique.htm](http://www.mccohi.com/oblique/oblique.htm).